Structure, Bonding, and Tyrosinase-Like Reactivity of Copper Complexes Coordinated by Mononucleating Tridentate N−O−N Type Ligands

Yen-Ting Cheng,[a] Hsiao-Lan Chen,[a] Shiou-Yuan Tsai,[a] Chan-Cheng Su,*[a] Huan-Sheng Tsang,[a] Ting-Shen Kuo,[a] Yi-Chou Tsai,[b] Fen-Ling Liao,[b] and Sue-Lein Wang[b]

Keywords: Enzyme models / N,O ligands / Copper / Oxidations

Copper complexes with mononucleating tridentate ligands of the N–O–N type, including 1,3-bis(benzimidazol-2-yl)-2-oxapropane (bbmo), 1,3-bis(*N*-methylbenzimidazol-2-yl)-2-oxapropane (bb^{Me}mo), 1,3-bis(*N*-*n*-propylbenzimidazol-2-yl)-2-oxapropane (bb^{Pr}mo), and 1,3-bis(pyrid-2-yl)-2-oxapropane (bpmo), were tested for the oxygenation of phenols. Mixed ligand copper complexes of [Cu(N–O–N)(N–N)](ClO$_4$)$_2$, where N–N denotes 2,2′-bipyridine (bipy), 1,10-phenanthroline (phen), ethylenediamine (en), and/or *N*,*N*,*N*′,*N*′-tetramethylethylenediammine (tmen), were prepared and characterized by elemental analyses, and electronic, vibrational, and epr spectroscopic measurements. The molecular structures of *fac*-[Cu(bb^{Me}mo)(bipy)(H$_2$O)](ClO$_4$)$_2$(H$_2$O) (**1a**), *fac*-[Cu(bb^{Me}mo)(phen)](ClO$_4$)$_2$(CH$_3$CN) (**4a**), *fac*-[Cu(bb^{Pr}mo)(phen)](ClO$_4$)$_2$ (**5a**), and *fac*-[Cu(bpmo)(bipy)(ClO$_4$)](ClO$_4$) (**7a**) were determined by X-ray diffraction methods. The structures of these complexes are square pyramids or elongated octahedra with the heterocycle nuclei forming the basal or equatorial planes. The terminal heterocycles of the facially coordinated tridentate ligands are nearly perpendicular to the basal or equatorial planes. Similar structures are proposed for the remaining complexes, based on spectroscopic data. Both stoichiometric and catalytic oxidation reactions of 2,4-di-*tert*-butylphenol and 2,4-di-*tert*-butylphenolate with dioxygen adducts of [Cu(bb^{Pr}mo)]$^+$ at room temperature afforded 3,3′,5,5′-tetra-*tert*-butyl-2,2′-biphenol and 3,5-di-*tert*-butyl-*o*-quinone. Similar reactions with the dioxygen adduct of [Cu(bpmo)]$^+$ yielded only 3,3′,5,5′-tetra-*tert*-butyl-2,2′-biphenol. In light of the tyrosinase-like reactivity, the possible intermediates, [(bb^{Pr}mo)$_2$Cu$_2$(μ-η^2:η^2-peroxo)]$^{2+}$, [(bb^{Pr}mo)$_2$Cu$_2$(μ-oxo)$_2$]$^{2+}$, and [(bpmo)$_2$Cu$_2$(μ-oxo)$_2$]$^{2+}$ are proposed.

Introduction

Tyrosinase and hemocyanins represent type 3 copper proteins that have been extensively characterized.[1−3] Their dicopper active sites bind dioxygen via the redox process, 2 Cu^{I} + O$_2$ → Cu^{II}(O$_2^{2-}$)Cu^{II}, to form (μ-η^2:η^2-peroxo)dicopper(II) units.[4] The formation of (μ-η^2:η^2-peroxo)dicopper(II) cores is likely governed by enclosure by the bulky protein residues and by the bonding capability of the three-coordinated imidazoles of the histidine residues to each copper. These peroxo units may be further involved in O$_2$ activation, via the *o*-hydroxylation of the phenol of tyrosine by tyrosinase, or take the reverse process, functioning as O$_2$ carriers in hemocyanins. To date some well-characterized peroxodicopper(II) complexes have been reported involving ligands with heterocycles other than imidazole,[5−8] or even without heterocycles.[9−14] Although these complexes are generally not stable at room temperature in contrast to their biological counterparts, they can be used as models to mimic the structures and/or functions of the active centers of the native systems. Among the three classes of synthetic peroxodicopper(II) complexes shown in Scheme 1,[15] μ-η^2:η^2-peroxodicopper(II) behaves differently from the other two and has a nonbasic or electrophilic reactivity.[16−18] Depending on the specific ligand, steric bulk, counterion, and solvent effects, μ-η^2:η^2-peroxodicopper(II) complexes have been shown to be in equilibrium with the isoelectronic bis(μ-oxo)dicopper(III) species.[11,19−23] Their substrate reactivities are different. The μ-η^2:η^2-peroxodicopper(II) favors oxygen atom transfer reactions,[18] while the bis(μ-oxo)dicopper(III) prefers hydrogen atom abstraction.[24] The oxidation reactions of phenolates with μ-η^2:η^2-peroxodicop-

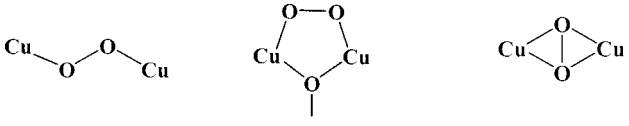

trans-μ-1,2-peroxo *cis*-1,2-peroxo μ-η^2 : η^2-peroxo

Scheme 1. Types of peroxodicopper(II) species

[a] Department of Chemistry, National Taiwan Normal University, Taipei 11718, Taiwan, ROC
Fax: (internat.) + 996-29324249
E-mail: chefv003@scc.ntnu.edu.tw
[b] Department of Chemistry, National Tsing Hua University, Hsinchu, Taiwan, ROC

  DOI: 10.1002/ejic.200300636

per(II) mainly afford catechols and *o*-quinones,[25] whereas similar reactions of phenols with bis(μ-oxo)dicopper(III) give rise to biphenols.[26]

In this report we describe the structures and substrate reactivity of a class of copper complexes coordinated by mononucleating tridentate ligands of N−O−N type, including 1,3-bis(benzimidazol-2-yl)-2-oxapropane (bbmo), 1,3-bis(*N*-methylbenzimidazol-2-yl)-2-oxapropane ($bb^{Me}mo$), 1,3-bis(*N*-*n*-propylbenzimidazol-2-yl)-2-oxapropane ($bb^{Pr}mo$), and 1,3-bis(pyrid-2-yl)-2-oxapropane (bpmo). The oxidation reactions of 2,4-di-*tert*-butylphenol and 2,4-di-*tert*-butylphenolate with dioxygen in the presence of stoichiometric or catalytic amounts of $[Cu(bb^{Pr}mo)]^+$ or $[Cu(bpmo)]^+$ at room temperature resulted in the generation of 3,3′,5,5′-tetra-*tert*-butyl-2,2′-biphenol and/or 3,5-di-*tert*-butyl-*o*-quinone, inferring the formation of bis(μ-oxo)dicopper(III) and/or (μ-η^2:η^2-peroxo)dicopper(II) intermediates during the reactions. The purpose of this report is to elucidate the conformation and coordination properties of the N−O−N tridentate ligands in order to reveal their roles in the peroxodicopper(II)/bis(μ-oxo)dicopper(III) equilibrium and substrate reactivity.

Results and Discussion

Synthesis of Complexes

The mixed-ligand complexes, $[Cu(bbmo)(LL)]^{2+}$, $[Cu(bb^{Me}mo)(LL)]^{2+}$, $[Cu(bb^{Pr}mo)(LL)]^{2+}$, and $[Cu(bpmo)(LL)]^{2+}$ (LL = phen and/or bipy), were prepared by the addition of one equivalent of the bidentate ligand, phen or bipy, to a 1:1 mixture of Cu^{II} perchlorate and the tridentate ligand, bbmo, $bb^{Me}mo$, $bb^{Pr}mo$, or bpmo. Attempts to prepare the 1:1 complexes, $[Cu(N-O-N)]^{2+}$, by mixing equivalent amounts of the ligands and copper perchlorate were unsuccessful. Instead, the 1:2 complexes, $[Cu(N-O-N)_2]^{2+}$, were isolated. In the case of the en and tmen complexes, only $[Cu(bb^{Pr}mo)(en)](ClO_4)_2$ (**6**) and $[Cu(bpmo)(tmen)](ClO_4)_2$ (**9**) complexes were isolated in pure form. As evidenced from X-ray structure results (vide infra) and spectroscopic studies, the tridentate ligands bond to the central Cu^{II} ion in a facial conformation for all of the mixed ligand complexes, in agreement with the usual findings that the strong benzimidazole and pyridine donors tend to bind at the equatorial positions and the weak ether oxygen at the axial site for the Cu^{II} complexes.

X-ray Structures

fac-$[Cu(bb^{Me}mo)(bipy)(H_2O)](ClO_4)_2(H_2O)$ (1a), *fac*-$[Cu(bb^{Me}mo)(phen)](ClO_4)_2(CH_3CN)$ (4a), and *fac*-$[Cu(bb^{Pr}mo)(phen)](ClO_4)_2$ (5a)

The molecular structures of mixed ligand complexes **1a**, **4a**, and **5a** are shown in Figures 1, 2, and 3, respectively. Selected bond lengths and angles are listed in Table 1. These complexes are composed of discrete copper complex cations, perchlorate anions, and/or solvent molecules. In the case of complex **1a**, the copper cation binds a H_2O molecule at the axial site to complete an elongated octahedron, with the copper slightly above the equatorial plane, inclined toward the H_2O. The deviations from the best equatorial plane of CuN_4 are Cu(1) +0.1709 Å, N(1) −0.1320 Å, N(2) +0.0499 Å, N(3) −0.1298 Å, and N(5) +0.0411 Å. The structures of the complex cations of **4a** and **5a** are square pyramidal [τ = 0.162 (**4a**); τ = 0.017 (**5a**)], because the perchlorate ions are too far away from the central copper ions. The deviations from the best basal plane of CuN_4 are Cu(1) +0.0467 Å, N(1) −0.0358 Å, N(2) +0.0136 Å, N(3) −0.0351 Å, and N(5) +0.0106 Å for **4a**, Cu(1) +0.0101 Å, N(1) −0.0087 Å, N(2) +0.0039 Å, N(3) −0.0084 Å, and N(5) +0.0032 Å for **5a**. The complex cations contain a facial $bb^{Me}mo$ or $bb^{Pr}mo$, with an elongated axial Cu−O of 2.570(4) Å for **1a**, 2.520(3) Å for **4a**, and 2.527(4) Å for **5a**. The fact that these axial Cu−O distances are significantly shorter than the corresponding axial Cu−N of 2.597(6) Å for the *trans*-*fac*-$[Cu(bbmn)_2](ClO_4)_2(H_2O)_2$ complex[27] (bbmn = 1,3-bis(benzimidazol-2-yl)-2-azapropane) is unexpected. The mean Cu−N distances and the intraligand ∠N−Cu−N angles of the tridentate ligands are 1.984±0.004 Å and 91.6(2)° for **1a**, 1.981±0.004 Å and 89.8(1)° for **4a**, and 1.995±0.006 Å and 88.1(2)° for **5a**. The mean bite angles of the five-member chelates of the tridentate ligands are 73.3±0.3° for **1a**, 75.6±0.2° for **4a**, and 75.6±0.2° for **5a**. The benzimidazole nuclei of these complexes lie nearly perpendicular to the CuN_4 basal or equatorial plane, with dihedral angles of 94.6° and 111.7° for **1a**, 89.4° and 105.9° for **4a**, and 86.5° and 93.5° for **5a**. All these geometric figures are analogous to those reported for *trans*-*fac*-$[Cu(bbmn)_2](ClO_4)_2(H_2O)_2$[27] (mean Cu−N of 2.010±0.008 Å; intraligand ∠N−Cu−N of 88.1°; mean bite angle of the five-member chelates ∠N−Cu−N of 74.9±0.4°), suggesting that the coordination capabilities of

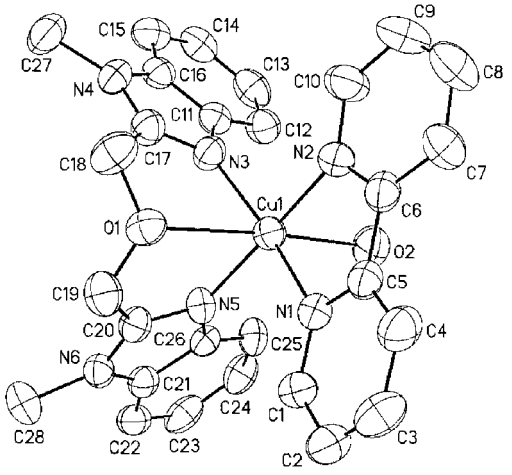

Figure 1. ORTEP diagram of *fac*-$[Cu(bb^{Me}mo)(bipy)(H_2O)](ClO_4)_2(H_2O)$ (**1a**); perchlorates, H_2O, and hydrogen atoms have been omitted for clarity

the tridentate ligands of these mixed ligand complexes are similar.

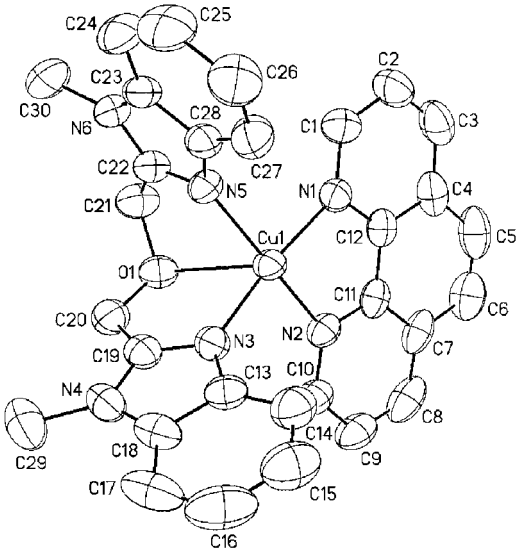

Figure 2. ORTEP diagram of *fac*-[Cu(bb^{Me}mo)(phen)]-$(ClO_4)_2(CH_3CN)$ (**4a**); perchlorates, CH_3CN, and hydrogen atoms have been omitted for clarity

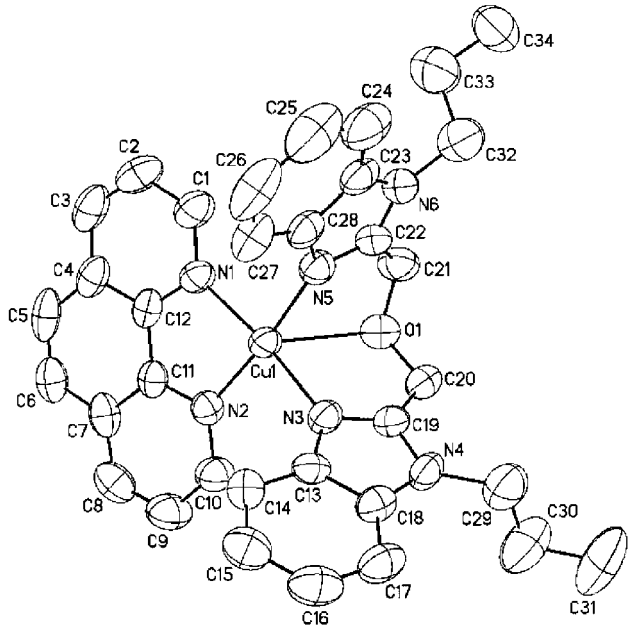

Figure 3. ORTEP diagram of *fac*-[Cu(bb^{Pr}mo)(phen)]$(ClO_4)_2$ (**5a**); perchlorates and hydrogen atoms have been omitted for clarity

It is interesting to note that the mean Cu−N bond lengths of 2.010±0.016 Å and the bite angles of 81.3±0.5° for the diimine ligands of these three complexes are also very similar, indicative of similar bonding abilities of the diimine ligands. Although the thermal vibrations are somewhat large for some oxygen atoms of the perchlorates, the bond lengths and angles of these complexes are in the normal ranges.[27−29] The largest difference peaks of 1.108 for **1a** and 1.281 for **5a** appear near the Cl(1) atom for **1a** and Cl(2) for **5a**, respectively.

Table 1. Selected bond lengths (Å) and angles (°) for complexes **1a**, **4a**, **5a**, and **7a**

fac-[Cu(bb^{Me}mo)(bipy)(H_2O)]$(ClO_4)_2(H_2O)$ (**1a**)

Cu(1)−N(1) 2.022(4)	Cu(1)−N(2) 2.013(4)
Cu(1)−N(3) 2.000(4)	Cu(1)−N(5) 1.989(4)
Cu(1)−O(1) 2.527(4)	Cu(1)−O(2) 2.368(4)
N(1)−Cu(1)−N(2) 80.8(2)	N(1)−Cu(1)−N(3) 162.3(2)
N(1)−Cu(1)−N(5) 94.7(2)	N(2)−Cu(1)−N(3) 94.3(2)
N(2)−Cu(1)−N(5) 172.0(2)	N(3)−Cu(1)−N(5) 88.1(2)
N(1)−Cu(1)−O(1) 88.0(2)	N(2)−Cu(1)−O(1) 97.7(2)
N(3)−Cu(1)−O(1) 75.8(2)	N(5)−Cu(1)−O(1) 75.4(2)
N(1)−Cu(1)−O(2) 91.4(2)	N(2)−Cu(1)−O(2) 86.5(2)
N(3)−Cu(1)−O(2) 105.3(2)	N(5)−Cu(1)−O(2) 100.3(2)
O(1)−Cu(1)−O(2) 175.5(2)	

fac-[Cu(bb^{Me}mo)(phen)]$(ClO_4)_2(CH_3CN)$ (**4a**)

Cu(1)−N(1) 2.020(4)	Cu(1)−N(2) 2.006(3)
Cu(1)−N(3) 1.979(3)	Cu(1)−N(5) 2.000(3)
Cu(1)−O(1) 2.529(3)	
N(1)−Cu(1)−N(2) 81.8(2)	N(1)−Cu(1)−N(3) 173.0(1)
N(1)−Cu(1)−N(5) 93.0(1)	N(2)−Cu(1)−N(3) 93.9(2)
N(2)−Cu(1)−N(5) 167.7(1)	N(3)−Cu(1)−N(5) 92.2(2)
N(1)−Cu(1)−O(1) 111.7(1)	N(2)−Cu(1)−O(1) 97.4(1)
N(3)−Cu(1)−O(1) 74.3(1)	N(5)−Cu(1)−O(1) 74.0(2)

fac-[Cu(bb^{Pr}mo)(phen)]$(ClO_4)_2$ (**5a**)

Cu(1)−N(1) 2.016(4)	Cu(1)−N(2) 2.005(4)
Cu(1)−N(3) 1.980(4)	Cu(1)−N(5) 1.987(4)
Cu(1)−O(1) 2.570(4)	
N(1)−Cu(1)−N(2) 81.4(2)	N(1)−Cu(1)−N(3) 173.3(2)
N(1)−Cu(1)−N(5) 93.2(2)	N(2)−Cu(1)−N(3) 93.7(2)
N(2)−Cu(1)−N(5) 174.3(2)	N(3)−Cu(1)−N(5) 91.6(2)
N(1)−Cu(1)−O(1) 112.5(2)	N(2)−Cu(1)−O(1) 110.7(2)
N(3)−Cu(1)−O(1) 73.5(2)	N(5)−Cu(1)−O(1) 73.0(2)

fac-[Cu(bpmo)(bipy)(ClO_4)](ClO_4) (**7a**)

Cu(1)−N(1) 2.031(4)	Cu(1)−N(2) 2.028(4)
Cu(1)−N(3) 2.003(4)	Cu(1)−N(4) 1.994(4)
Cu(1)−O(1) 2.323(4)	Cu(1)−O(2) 2.417(4)
N(1)−Cu(1)−N(2) 85.8(2)	N(1)−Cu(1)−N(3) 174.3(2)
N(1)−Cu(1)−N(4) 97.0(2)	N(2)−Cu(1)−N(3) 95.0(2)
N(2)−Cu(1)−N(4) 172.5(2)	N(3)−Cu(1)−N(4) 81.6(2)
N(1)−Cu(1)−O(1) 79.3(2)	N(2)−Cu(1)−O(1) 79.0(2)
N(3)−Cu(1)−O(1) 95.3(2)	N(4)−Cu(1)−O(1) 94.6(2)
N(1)−Cu(1)−O(2) 89.7(2)	N(2)−Cu(1)−O(2) 98.1(2)
N(3)−Cu(1)−O(2) 95.8(2)	N(4)−Cu(1)−O(2) 89.0(2)
O(1)−Cu(1)−O(2) 168.8(2)	

fac-[Cu(bpmo)(bipy)(ClO_4)](ClO_4) (7a)

The molecular structure of **7a** is shown in Figure 4. Selected bond lengths and angles are listed in Table 1. The discrete elongated octahedral copper(II) complex cation comprises a facial bpmo, an equatorial bipy, and a perchlorate anion at the axial site. The deviations from the best equatorial plane of CuN_4 are Cu(1) +0.088 Å, N(1) −0.012 Å, N(2) −0.033 Å, N(3) −0.010 Å, and N(4) −0.033 Å. The facial bpmo has a mean Cu−N distance of 2.030±0.002 Å,

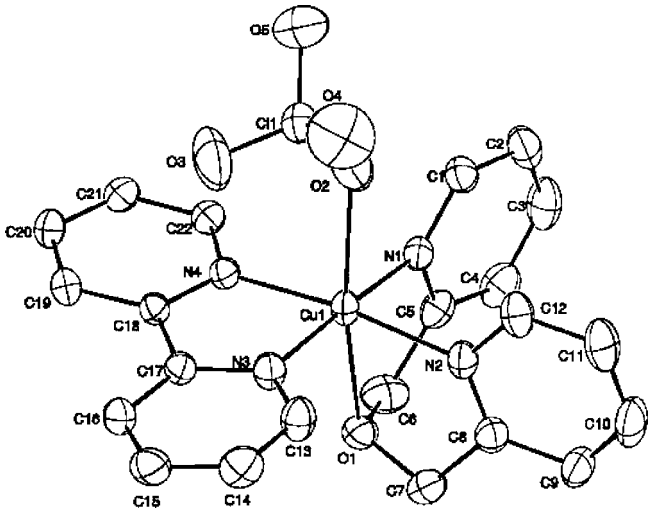

Figure 4. ORTEP diagram of *fac*-[Cu(bpmo)(bipy)(ClO_4)](ClO_4) (**7a**); one perchlorate and hydrogen atoms have been omitted for clarity

which is slightly longer than that of complex **1a** of 1.984±0.004 Å. However, the axial Cu−O of 2.323(4) Å of the bpmo is shorter than that of complex **1a** of 2.570(4) Å. It is likely that the bonding ability of the pyridine nucleus in bpmo is weaker than that of the benzimidazole nucleus.

Table 2. EPR spectroscopic data for bbmo, $bb^{Pr}mo$, $bb^{Me}mo$, and bpmo Cu^{II} complexes[a]

$g_{\|}$	$g_{\perp}$	$A_{\|}$(Cu)	$A_{\perp}$(Cu)	$A_{\perp}$(N)	$A_{\perp}$(N′)[b]	
[Cu($bb^{Pr}mo$)(en)](ClO_4)$_2$ (**6**)						
2.232	(2.052 2.013)[c]	197				Powder
2.269	2.086	184	17	17	16	dmf glass
[Cu(bpmo)(tmen)](ClO_4)$_2$ (**9**)						
2.216	2.066					Powder
2.259	2.082	182	17	17	14	dmf glass
[Cu($bb^{Me}mo$)(bipy)](ClO_4)$_2$ (**1**)						
2.214	2.060	190				Powder
2.289	2.084	184	17	17	16	dmf glass
[Cu($bb^{Pr}mo$)(bipy)](ClO_4)$_2$(H_2O) (**2**)						
2.260	(2.073 2.008)[c]					Powder
2.286	2.084	184	17	17	16	dmf glass
[Cu(bbmo)(bipy)](ClO_4)$_2$(CH_3CN)$_{0.5}$ (**3**)						
2.249	(2.166 2.067)[c]	181				Powder
2.288	2.085	184	17	17	14	dmf glass
[Cu(bpmo)(bipy)](ClO_4)$_2$(H_2O)$_{0.5}$ (**7**)						
[d]	2.070					Powder
2.277	2.085	182	18	17	14	dmf glass
[Cu($bb^{Me}mo$)(phen)](ClO_4)$_2$(H_2O)$_3$ (**4**)						
2.230	2.057	174				Powder
2.293	2.086	184	17	17	16	dmf glass
[Cu($bb^{Pr}mo$)(phen)](ClO_4)$_2$(H_2O)$_2$ (**5**)						
2.251	(2.073 2.008)[c]	166				Powder
2.291	2.085	184	17	17	15	dmf glass
[Cu(bpmo)(phen)](ClO_4)$_2$(H_2O)$_{0.5}$ (**8**)						
2.233	2.066	185				Powder
2.279	2.084	183	17	17	15	dmf glass

[a] X-band EPR spectra measured at room temperature for powder samples, and at 77 K for glass. Hyperfine coupling constants in 10^{-4} cm^{-1}. [b] N′ denotes the second nitrogen. [c] Rhombic powder spestrum with g_y and g_x. [d] Not observed.

The pyridine nuclei of the bpmo lie nearly perpendicular to the CuN_4 equatorial plane, with dihedral angles of 89.6° and 92.9°. A comparison of the mean Cu−N bond lengths of bipy of 1.999±0.005 Å for **7a** with that of 2.010±0.016 Å for complex **1a** suggests that the bonding capability of the bipy is nearly equal in these two complexes. The bond lengths and angles of complex **7a** are in the normal ranges.

Spectroscopic Studies

Selected i.r. data are listed in the Experimental section. In the 3500 cm^{-1} region, broad O−H stretching absorption peaks appear for some of the complexes, suggesting the presence of H_2O. Two characteristic N−H stretching peaks at 3345 and 3283 cm^{-1} indicate the en ligand in (**6**). There are some characteristic vibration absorptions for the heterocycle nuclei including the C=N and C=C stretching at ca.1600 to 1480 cm^{-1}, aromatic C−H bending at ca. 740 cm^{-1}, and ring deformation at ca. 430 cm^{-1}. It is generally useful to account for the coordination of the perchlorate by counting the number of very strong ν(Cl−O) at ca. 1100 cm^{-1}. However, care must be exercised in elucidating the complexes with N−O−N tridentate ligands, because of the interference by the strong ν(C−O) peaks in the same region. For some complexes, the Cu−N stretching peaks in the ca. 300 cm^{-1} region are tentatively assigned.

Table 2 lists e.p.r. spectroscopic data of the compounds. The powder e.p.r. spectra of the axial or axial rhombic types of these complexes are consistent with square pyramidal and tetragonal structures and indicative of a $d_{x^2-y^2}$ or d_{xy} ground state.[30−31] For the glass spectra in dmf, CH_3OH/CH_3CN, or CH_3CN matrices, characteristic superhyperfine splittings were observed for all of the complexes. The g_z values are larger in dmf glass than in CH_3OH/CH_3CN or CH_3CN matrices, while the reverse is true for the A_z values. It is likely that the coordination of the axial ether oxygen of the tridentate ligand is replaced by the dmf molecule, consistent with the UV/Vis spectroscopic data (vide infra), and that the basal or equatorial plane is also slightly distorted toward a tetrahedron.[32]

Electronic spectroscopic data for the tridentate complexes are shown in Table 3. The reflectance LF spectra of the mixed-ligand complexes exhibit similar envelopes with a main peak at ca. 524 nm to ca. 710 nm and a pronounced shoulder or small peak on the low energy side of ca. 900 nm extending to ca. 1200 nm. In CH_3OH/CH_3CN or CH_3CN solution, these complexes show a peak at ca. 560 nm to ca. 610 nm with a shoulder at ca. 900 nm extending to 1200 nm, suggesting that the structures of the dissolved complexes are either square pyramidal or tetragonal, as are their solid counter species. The LF band maxima suggest that the bonding strengths of the N-donor ligands are consistent with their σ-donating capabilities, namely, amines are stronger than imines. However, it is noteworthy that the d-d bands (reflectance and acetonitrile solution) appear in general at higher energy region for bpmo complexes than the corresponding $bb^{R}mo$ (R = Pr, Me, and H) complexes. Because pyridine and benzimidazole have comparable basicities, the differences in the ligand field spectra are attribu-

Table 3. Electronic spectroscopic data for bbmo, bb^{Pr}mo, bb^{Me}mo, and bpmo Cu^{II} complexes

Compd.	Intraligand λ_{max} ($\varepsilon \times 10^3$), nm[a]	CT λ_{max} (ε), nm[a]	LF λ_{max} (ε), nm[a]
6/rflx.			570, 800 sh 1100 sh
6/MeOH[b]	252 (20.0), 257 (19.5), 273 (17.5), 279 (17.4), 285 sh (13.5)	337 (360)	570 (79)
6/dmf	273 (16.9), 279 (17.7), 287 (14.4)	322 sh (970)	586 (75)
9/rflx.			524, 623 sh
9/MeCN	259 (12.5)	300 sh (5700)	560 (76), 800 sh (16)
9/dmf			658 (87)
1/rflx.			638, 1100
1/MeCN[c]	244 (30.5), 274 (19.8), 281 (19.3), 302 (16.5), 312 (15.0)	363 sh (450)	605 (77), 950 (20)
1/dmf	275 (46.7), 288 (28.8), 300 sh (20)		640 (80), 950 sh (15)
2/rflx.			668 1100 sh
2/MeOH[b]	247 (32.8), 274 (25.0), 280 (24.7), 301 (17.8), 311 (16.0)	362 sh (530)	609 (78), 845 (24)
2/dmf	282 sh (29.2), 287 (29.8), 300 sh (21.5), 312 sh (17.3)		640 (87), 850 (31)
3/rflx.			670 1100
3/MeCN	240 (27.6), 273 (18.2), 280 (17.0), 302 (13.8), 312 (12.6)	364 sh (540)	600 (84), 987 sh (20)
3/dmf			623 (98)
7/rflx.			628
7/MeCN	231 sh (22.5), 256 (23.1), 273 sh (15.1), 301 (12.5), 312 (10.7)		605 (54), 850 sh (15)
7/dmf	300 (11.1), 312 (9.20)	382 sh (280)	645 (58), 900 sh (20)
4/rflx.			558, 630, 800 sh
4/MeCN[c]	235 sh (35.4), 250 sh (25.6), 273 (47.0), 295 sh (10.6)	368 sh (540)	605 (80), 900 sh (28)
4/dmf	282 (30.7), 288 (30.1), 300 sh	313 (11300), 417 (747)	663 (97), 950 sh (30)
5/rflx.			710 1100 sh
5/MeOH[b]	204 (132), 230 sh (48.6), 273 (61.3), 297 sh (14.6)	362 sh (550)	607 (75), 845 sh (14)
5/dmf	274 (54.5), 287 sh (32.5), 294 sh (18.2)	405 sh (410)	637 (83), 845 sh (25)
8/rflx.			633
8/MeCN	205 (47.3), 226 (40.5), 258 sh (36.5), 268 (36.9), 295 sh (9.93)		611 (53), 850 sh (14)
8/dmf	271 (36.0), 296 sh (10.9)	382 sh (292)	651 (57), 965 sh (14)
L1/MeOH	247 (13.5), 252 sh (13.3), 270 sh (12.1), 275 (15.8), 282 (14.5)		
L1/EtOH[d]	252 (13.8), 272 (17.0), 282 (15.1)		
L2/MeOH	253 sh (13.8), 258 (14.6), 272 sh (12.9), 278 (14.6), 287 (12.5)		
L3/MeOH	258 (17.4), 272 sh (14.9), 278 (16.3), 286 (13.4)		
L4/MeCN	256 sh (13.4), 260 (13.9), 266 sh (11.2)		

[a] ε in $M^{-1}cm^{-1}$. [b] MeOH/MeCN = 2:1. [c] Contains 10% MeOH. [d] Ref.[42]

table to the π-interactions between the copper d_π orbitals and the π orbitals of the heterocycles of the tridentate ligands.

The intraligand transitions for the N−O−N tridentate ligands are assigned in the ca. 245 nm to ca. 290 nm region. There are essentially no shifts of the π→π* transition peaks of the tridentate ligands for the en and tmen complexes as compared with those of the corresponding free ligand molecules. Despite some interference due to the diimine ligands, blue shifts of the π→π* transition peaks of the tridentate ligands were observed for the mixed-ligand bipy complexes, indicative of π interactions involved in the coordination bonds between the central copper and the heterocycles of the tridentate ligands.

While dissolving these complexes in dmf, the blue solution gradually turned green. The LF bands at ca. 600 nm were red-shifted by ca. 30 nm to ca. 40 nm, but not the low energy peak or shoulder. New CT bands were observed in the 300 nm region. These spectral changes indicate that the central ether oxygen atoms of the tridentate ligands are replaced by the dmf molecules, in agreement with the e.p.r. data (vide supra).

Oxidation of Phenols or Phenolates

The results of stoichiometric and catalytic oxidation reactions of DBP and phenolates, DBP−NEt_3, are summarized in Table 4. It is obvious that the N−O−N tridentate ligands are indispensable for the oxidation reactions, since no oxidized products were observed for the reactions of DBP with $[Cu(CH_3CN)_4]^+$ (entries 5 and 10).

In the stoichiometric reactions, both TBBP (3,3′,5,5′-tetra-*tert*-butyl-2,2′-biphenol) and DBQ (3,5-di-*tert*-butyl-*o*-quinone) were produced in nearly equal amounts for the reactions of DBP, and DBP−NEt_3 as well, with Cu(bb^{Pr}mo)−O_2 adduct in CH_2Cl_2 at 25 °C (entries 1 and 2). Although mechanistic studies[16−18] have indicated that the aromatic ligand hydroxylation involves an electrophilic attack on the arene ring by (μ-η^2:η^2-peroxo)dicopper(II) intermediate, most of the reported studies on the intermolecular oxidations of DBP with peroxo intermediate report TBBP as a major product.[15,23,33−35] Our results with high DBQ generation are in reasonably good agreement with the mechanistic studies, inferring the formation of (μ-η^2:η^2-peroxo)dicopper(II) and bis(μ-oxo)dicopper(III) intermediates supported by bb^{Pr}mo during the reactions. The reactions of DBP, and also DBP-NEt_3, with the Cu(bpmo)-O_2 adduct in CH_2Cl_2 at 25 °C (entries 3 and 4), however, generate only TBBP, implying the presence of a bis(μ-oxo)dicopper(III) intermediate. These reactions can also be carried out under catalytic conditions (entries 6−9). The catalytic reactions require a much longer reaction time (3 to 14 days), due to

Table 4. Oxidation reactions of DBP with O_2 in the presence of $Cu^I(N-O-N)$ complexes[a]

Entry[a]	N−O−N/substrate[b]	TBBP[c] (%)	DBQ[d] (%)	DBP[e] (%)
I. Stoichiometric reactions[f]				
1	$bb^{pr}mo$/DBP	45	42	10
2	$bb^{pr}mo$/DBP-NEt_3	43	44	10
3	bpmo/DBP	43	0	47
4	bpmo/DBP-NEt_3	10	0	59
5	$[Cu(MeCN)_4]^+$/DBP	0	0	75
II. Catalytic reactions[g]				
6	$bb^{pr}mo$/DBP[h]	68	6	20
7	$bb^{pr}mo$/DBP-NEt_3[h]	55	0	9
8	bpmo/DBP[i]	56	0	37
9	bpmo/DBP-NEt_3[i]	37	0	59
10	$[Cu(MeCN)_4]^+$/DBP[i]	trace	0	[j]

[a] The dioxygen adducts for the stoichiometric reactions were prepared by the reaction of O_2 with a solution of equimolar Cu^I and N−O−N at room temperature for 24 h. [b] DBP = 2,4-di-*tert*-butylphenol. DBP−NEt_3 = DBP/NEt_3 (1:1). [c] Isolated yield. TBBP = 3,3′,5,5′-tetra-*tert*-butyl-2,2′-biphenol. [d] Isolated yield. DBQ = 3,5-di-*tert*-butyl-*o*-quinone. [e] Recovered DBP. [f] Molar ratio of Substrate/Cu(N−O−N) = 1:1. The reactions were carried out in CH_2Cl_2 at 25 °C for 24 h. [g] Molar ratio of Substrate/Cu(N−O−N) = 1:0.01. The reactions were carried out in CH_2Cl_2 at 25 °C. [h] 14 days. [i] 3 days. [j] Not measured.

the small amount (one hundredth) of the copper catalyst employed, and the turn over numbers are in the order of 10^3.

The oxygenation reactions of phenolates to catechols by $[(\mu\text{-}\eta^2\text{:}\eta^2\text{-}O_2)Cu_2(L\text{-}66)]$[36−39] {L-66 = α,α′-bis{bis[2-(1-methyl-2-benzimidazolyl)ethyl]amino}-*m*-xylene} and by $[(\mu\text{-}\eta^2\text{:}\eta^2\text{-}O_2)Cu_2(L^{Py2Bz})_2]$[40] {$L^{Py2Bz}$ = *N*,*N*-bis[2-(2-pyridyl)ethyl]-α,α-dideuteriobenzylamine} have been demonstrated. The oxidation of 4MP-Li (lithium 4-methylphenolate) with Cu($bb^{Pr}mo$)−O_2 adduct afforded 3,5-di-*tert*-butyl-1,2-catechol in 37% isolated yield further assuring that the adduct is mainly ($\mu\text{-}\eta^2\text{:}\eta^2$-peroxo)dicopper(II). It is noteworthy that the copper complex with the mononucleating ligand, L-6 {*N*,*N*-bis[2-(1-methyl-2-benzimidazolyl)-ethyl]amine},[37] is inactive in the monooxygenase reaction. The reactivity with respect to oxygenation can be attributed to the conformations of the coordinated tridentate ligands. The L-6 ligand tends to coordinate to copper(II) in a meridional fashion, while N−O−N ligands, bb^Rmo and bpmo, should assume a facial conformation. Accordingly, it would be proper for $[Cu(N-O-N)]^+$ to accommodate a side-on O_2, but not $[Cu(L\text{-}6)]^+$.

Conclusion

The oxygenation reactions of DBP (2,4-di-*tert*-butylphenol) and DBP−NEt_3 (2,4-di-*tert*-butylphenolate) with the Cu($bb^{Pr}mo$)−O_2 adduct give rise to the production of DBTQ (3,5-di-*tert*-butyl-*o*-quinone). The same reaction of 4MP-Li (lithium 4-methylphenolate) produces 4-methyl-1,2-catechol. These tyrosinase-like reactions infer strongly the presence of $\mu\text{-}\eta^2\text{:}\eta^2$-peroxodicopper(II) intermediate supported by $bb^{Pr}mo$. The intermediate coordinated by $bb^{Pr}mo$ having a facial conformation is likely stabilized by π-interactions of the two perpendicularly oriented terminal benzimidazole nuclei, and tends to become stable at room temperature. Further investigation on π-interactions is currently in progress.

Experimental Section

General Remarks: Electronic spectra were recorded on a Hitachi U-3501 spectrophotometer equipped with an integrating sphere for reflectance measurements. IR spectra were recorded as Nujol mulls on a BIO-RAD FTS-40 FTIR spectrometer and a JASCO FT/IR 700 spectrometer. Nuclear magnetic resonance (NMR) spectra were recorded with Varian Gemini 2000 (200 MHz) and Bruker AV-400 (400 MHz) spectrometers. EPR spectra were obtained by using a Bruker EMX 10 spectrometer. The EPR simulations were performed using WINEPR SimFonia program. Mass spectra were acquired on a Finnigan TSQ 700 spectrometer. Elemental analyses were carried out by the microanalysis laboratories of National Chung-Hsin University, Taichung, Taiwan.

Preparation of Ligands

bbmo (L1):[41] Diglycolic acid (6.05 g, 45 mmol) and *o*-phenylenediamine (9.75 g, 90 mmol) in 4 N HCl solution (250 mL) were refluxed for 14 h. After cooling to room temperature, the precipitates were filtered and then dissolved in hot H_2O. The aqueous solution was neutralized with conc. NH_4OH. The precipitates were filtered and dissolved in CH_3OH and treated with activated carbon to afford white products. Yield 72%. mp, 280 °C. MS (EI): *m*/*z* = 279 [M + 1] (100). ^1H NMR (200 MHz [D_6]DMSO): δ = 4.87 (s, 4 H, CH_2), 7.23−7.17 (m, 4 H, benzimidazolyl-5,6-*H*), 7.59−7.54 (m, 4 H, benzimidazolyl-4,7-*H*) ppm. {^1H NMR, ([D_6]DMSO): δ = 4.95 (s, 4 H), 7.3 (m, 4 H), 7.7 (m, 4 H) ppm[42]}; {^1H NMR (CD_3OD): δ = 4.95 (s, 4 H), 7.15 (m, 4 H), 7.7 (m, 4 H) ppm[41]}. IR (cm^{-1}): ν(C=C, C=N) 1623 mw, 1587 mw, 1533 mw, 1465 s, ν(C−O) 1102 s, 1039 m, δ(CH, bim) 768 m, 748 s, δ(bim) 434 mw.

$bb^{Me}mo$ (L2): This compound was prepared similarly as bbmo but using *N*-methyl-*o*-phenylenediamine. Yield 65%. mp, 174 °C. MS (FAB^+): *m*/*z* = 307 [M + 1] (40). ^1H NMR (400 MHz, $CDCl_3$): δ = 3.81 (s, 6 H, CH_3), 4.93 (s, 4 H, CH_2), 7.34−7.28 (m, 4 H, benzimidazolyl-5,6-*H*), 7.77−7.75 (m, 4 H, benzimidazolyl-4,7-*H*) ppm. IR (cm^{-1}): ν(C=C, C=N) 1615 mw, 1506 w, 1475 s, ν(C−O) 1081 s, 1021 m, δ(CH, bim) 771 ms, 756 s, 747 s, δ(bim) 411 w.

$bb^{Pr}mo$ (L3):[43] Powdered KOH (1.40 g, 25 mmol) was added to a stirred suspension of 1,3-bis(benzimidazol-2-yl)-2-oxapropane (1.39 g, 5 mmol) in acetone (10 mL). After 20 min, iodopropane (1.70 g, 10 mmol) of was added to the white cloudy reaction mixture. After stirring at room temperature for 2 h, the orange reaction mixture was transferred to a separating funnel containing benzene (100 mL). The organic layer was washed with water (1 × 20 mL) and saturated sodium chloride solution (20 mL) and was dried with $MgSO_4$ (5 g). The filtered organic solution was rotary evaporated and then added with diethyl ether to give white precipitates. Yield 70%. Mp, 79 °C. MS (FAB^+): *m*/*z* = 363 [M + 1] (100). ^1H NMR (400 MHz, [D_6]DMSO): δ = 0.79 (t, *J* = 7 Hz, 3 H, CH_3), 1.69 (h, *J* = 7 Hz, 2 H, CH_2), 4.20 (t, *J* = 7 Hz, 2 H, CH_2), 4.87 (s, 4 H, CH_2), 7.22−7.17 (m, 4 H, benzimidazolyl-5,6-*H*), 7.59−7.54 (m, 4 H, benzimidazolyl-4,7-*H*) ppm. IR (cm^{-1}): ν(C=C, C=N) 1667 s, 1614 s, 1515 ms, ν(C−O) 1089 s, 1007 s, δ(CH, bim) 743 s, δ(bim) 434 mw.

bpmo (L4):[44] 2-(Hydroxymethyl)pyridine (2.89 g, 25.9 mmol) was added to a solution of NaH (60%, 2.10 g, 52.5 mmol) in DMF (75 mL). The solution was stirred at 40 °C for 2 h and then cooled to room temperature. 2-(Bromomethyl)pyridine hydrobromide (6.48 g, 25.6 mmol) was added to a DMF solution (50 mL) of NaH (60%, 1.35 g, 33.7 mmol), and stirred at room temperature for 2 h. The solutions were mixed, heated at 70 °C for 2 h, and then quenched by adding H_2O (10 mL). Both H_2O and DMF were removed by vacuum distillation. The residue was dissolved in H_2O (100 mL) and extracted with diethyl ether (2 × 100 mL). The organic extract was rotary evaporated to give yellow products. Yield 22%. MS (FAB^+): *m/z* = 201.06 [M + 1] (100). ^1H NMR (400 MHz, $CDCl_3$): δ = 4.81 (s, 4 H, C*H*$_2$), 7.22 (t, *J* = 7 Hz, 2 H, pyridyl-4-*H*), 7.55 (d, *J* = 8 Hz, 2 H, pyridyl-3-*H*), 7.74 (t, *J* = 7 Hz, 2 H, pyridyl-5-*H*), 8.58 (d, *J* = 4 Hz, 2 H, pyridyl-6-*H*) ppm. IR (cm^{-1}): ν(C=C, C=N) 1634 m, 1591 s, ν(C−O) 1117 s, δ(CH, py) 755 s, δ(py) 425 mw.

Preparation of Complexes

[Cu(bb^{Me}mo)(bipy)](ClO$_4$)$_2$ (1): To a stirred CH_3OH solution (5 mL) of $Cu(ClO_4)_2·6H_2O$ (741 mg, 2 mmol), a solution of bb^{Me}mo (612 mg, 2 mmol) in CH_3OH (10 mL) was added. After reaction at room temperature for 2 h, a solution of bipy (313 mg, 2 mmol) in CH_3OH (10 mL) was added dropwise to the cloudy green solution and the reaction solution was stirred for another 2 h. The blue products were filtered and dried under vacuum. Yield 90%. M.p. 246 °C (dec.); found C 46.71, H 3.37, N 11.20. $C_{28}H_{26}Cl_2CuN_6O_9$: calcd. C 46.39, H 3.61, N 11.59%. IR (cm^{-1}): ν(C=C, C=N) 1605 m, 1508 s, 1500 s, ν(ClO_4^-) 1094 vs br., 623 s, ν(C−O) 1048 s, 1033 s, δ(CH, bipy) 784 ms, δ(CH, bim) 772 ms, 763 ms, 753 ms, δ(bim) 432 w, ν(Cu−N) 345 w, 304 mw, 282 mw. The purple crystals, *fac*-[Cu(bb^{Me}mo)(bipy)(H_2O)](ClO$_4$)$_2$(H_2O) (**1a**), suitable for X-ray diffraction were obtained by slow diffusion of diethyl ether to a dmf solution.

[Cu(bb^{Pr}mo)(bipy)](ClO$_4$)$_2$(H_2O) (2): This blue complex was prepared similarly as the previous complex but using bb^{Pr}mo and was recrystallized from CH_3CN and diethyl ether. Yield 42%. M.p. 240 °C (dec.); found C 48.05, H 4.22, N 10.80. $C_{32}H_{36}Cl_2CuN_6O_{10}$: calcd. C 48.10, H 4.54, N 10.52%. IR (cm^{-1}): ν(O−H) 3562 m br., ν(C=C, C=N) 1610 s, 1605 s, 1567 m, 1503 s, 1495 s, ν(ClO_4^-) 1081 vs br., 623 s, δ(CH, bipy) 767 s br., δ(CH, bim) 730 s, δ(bim) 438 w, δ(bipy) 415w.

[Cu(bbmo)(bipy)](ClO$_4$)$_2$(CH_3CN)$_{0.5}$ (3): This blue complex was prepared similarly as the previous complex but using bbmo and was recrystallized from CH_3CN/CH_3OH (1:1) and diethyl ether. Yield 81%. M.p. 234 °C (dec.); found C 45.08, H 3.15, N 12.60. $C_{27}H_{23.5}Cl_2CuN_{6.5}O_9$: calcd. C 45.19, H 3.28, N 12.69% IR (cm^{-1}): ν(N−H) 3274 m br., ν(C=C, C=N) 1612 m, 1603 m, 1540 w, 1498 m, ν(ClO_4^-) 1093 vs br., 622 s, δ(CH, bipy) 770 ms, δ(CH, bim) 752 s, 743 s, δ(bim) 431 w, ν(Cu−N) 330 w, 304 w, 292 mw, 282 mw.

[Cu(bb^{Me}mo)(phen)](ClO$_4$)$_2$(H_2O)$_3$ (4): This blue complex was prepared similarly as the previous complex but using bb^{Me}mo and phen. Yield 90%. M.p. 232 °C (dec.); found C 45.17, H 3.87, N 10.42. $C_{30}H_{32}Cl_2CuN_6O_{12}$: calcd. C 44.87, H 4.01, N 10.46%. IR (cm^{-1}): ν(OH) 3625w br, 3400w br, ν(C=C, C=N) 1610 mw, 1591 mw, 1542 mw, 1508 m, ν(ClO_4^-) 1091 vs br., 624 s, ν(C−O) 1044 m sh, 1012 mw, δ(CH, phen) 852 ms, δ(CH, bim) 757 s, 750 ms, 745 ms, δ(bim) 432 mw, ν(Cu−N) 341 mw, 312 mw, 282 mw. The blue crystals, *fac*-[Cu(bb^{Me}mo)(phen)](ClO$_4$)$_2$(CH_3CN) (4**a**), suitable for X-ray diffraction were obtained by slow diffusion of diethyl ether to an acetonitrile solution.

[Cu(bb^{Pr}mo)(phen)](ClO$_4$)$_2$(H_2O)$_2$ (5): This green complex was prepared similarly as the previous complex but using bb^{Pr}mo. Yield 51%. M.p. 242 °C (dec.); found C 48.33, H 4.16, N 10.35. $C_{34}H_{38}Cl_2CuN_6O_{11}$: calcd. C 48.55, H 4.55, N 9.99%. IR (cm^{-1}): ν(OH) 3564 w br., ν(C=C, C=N) 1610 mw. 1590 mw. 1521 m. 1495 s, ν(ClO_4^-) 1101 vs br., 623 s, ν(C−O) 1040 m sh. 1005 mw, δ(CH, phen) 850 ms, δ(CH, bim) 763 s. 740 m. 720 s, δ(bim) 437 mw. The purple crystals, *fac*-[Cu(bb^{Pr}mo)(phen)](ClO$_4$)$_2$ (**5a**), suitable for X-ray diffraction were obtained by slow diffusion of diethyl ether to a dmf solution.

[Cu(bb^{Pr}mo)(en)](ClO$_4$)$_2$ (6): This purple complex was prepared similarly as the previous complex but using bb^{Pr}mo and en. Yield 55%. M.p. 226 °C (dec.); found C 42.04, H 5.02, N 11.95. $C_{24}H_{34}Cl_2CuN_6O_9$: calcd. C 42.08, H 5.00, N 12.27%. IR (cm^{-1}): ν(NH) 3345 ms, 3283 ms, ν(C=C, C=N) 1611 m, 1594 s, 1503 s, 1496 s, ν(ClO_4^-) 1107 vs br., 626 s, ν(C−O) 1035 s sh, 1050 s, δ(CH, bim) 800 m, 765 s, 705 m, δ(bim) 435 mw.

[Cu(bpmo)(bipy)](ClO$_4$)$_2$(H_2O)$_{0.5}$ (7): This blue complex was prepared similarly as the previous complex but using bpmo and bipy. Yield 75%. M.p. 206 °C (dec.); found C 41.76, H 2.99, N 8.96. $C_{22}H_{21}Cl_2CuN_4O_{9.5}$ calcd. C 42.09, H 3.37, N 8.92%. IR (cm^{-1}): ν(OH) 3442 ms br., ν(C=C, C=N) 1606 s, 1573 m, ν(ClO_4^-) 1098 vs br., 623 s, ν(C−O) 1030 s, 985 m, δ(CH, bipy) 775 s, δ(CH, py) 765 s sh, 730 s, δ(py) 420 mw. The blue crystals, *fac*-[Cu(bpmo)(bipy)(ClO$_4$)](ClO$_4$) (**7a**), suitable for X-ray diffraction were obtained by slow diffusion of diethyl ether to an acetonitrile solution.

[Cu(bpmo)(phen)](ClO$_4$)$_2$(H_2O)$_{0.5}$ (8): This blue complex was prepared similarly as the previous complex but using bpmo and phen. Yield 74%. M.p. 201 °C (dec.); found C 44.11, H 3.34, N 8.25. $C_{24}H_{21}Cl_2CuN_4O_{9.5}$ calcd. C 44.22, H 3.24, N 8.59%. IR (cm^{-1}): ν(OH) 3600 w br., 3445 w br., ν(C=C, C=N) 1633 m, 1608 ms, 1586 m, 1520 ms, ν(ClO_4^-) 1092 vs br., 623 s, ν(C−O) 1052 m, 1008 w, δ(CH, phen) 853 ms, δ(CH, py) 782 m, 762 ms, δ(py) 434 mw.

[Cu(bpmo)(tmen)](ClO$_4$)$_2$ (9): This purple complex was prepared similarly as the previous complex but using bpmo and tmen. Yield 38%. M.p. 78 °C; found C 37.70, H 5.03, N 10.13. $C_{18}H_{28}Cl_2CuN_4O_9Cl_2$: calcd. C 37.35, H 4.84, N 9.68%. IR (cm^{-1}): ν(C=C, C=N) 1609 m, 1573 w, ν(ClO_4^-) 1093 vs br., 623 s, ν(C−O) 1164 m, δ(CH, py) 770 s, δ(py) 424 w.

Oxidation of Phenol or Phenolate with Peroxodicopper(II) and/or Bis(μ-oxo)dicopper(III): The μ-η^2:η^2-peroxodicopper(II) and/or bis(μ-oxo)dicopper(III) intermediates were generated by the reaction of [Cu(CH_3CN)$_4$](ClO$_4$) (185 mg, 0.56 mmol) and tridentate ligand (0.56 mmol) in CH_2Cl_2/CH_3CN (8:2, 10 mL) with O_2 at room temperature overnight. After removal of excess O_2 by bubbling N_2 gas into the solution for 15 min, a solution of DBP (117 mg, 0.56 mmol) with or without NEt_3 (0.56 mmol) in CH_2Cl_2 (5 mL) was added into the solution by cannulation. The mixture was stirred under N_2 at room temperature for 24 h. After evaporation of the solvent, the residue formed was columned on silica gel (ethyl acetate/hexane, 1:8), affording 3,3′,5,5′-tetra-*tert*-butyl-2,2′-biphenol, 3,5-di-*tert*-butyl-*o*-quinone, and the starting 2,4-di-*tert*-butylphenol. The oxygenation of 4MP-Li (lithium 4-methylphenolate) was carried out similarly in acetone, yielding 4-methylcatechol.[40]

Catalytic Oxidation of 2,4-Di-*tert*-butylphenol (DBP) or 2,4-Di-*tert*-butylphenolate (DBP-NEt$_3$) in the Presence of Copper(I) Complexes of bb^{Pr}mo or bpmo: A CH_2Cl_2 solution (10 mL) of 2,4-di-*tert*-butylphenol (1.65 g, 7.98 mmol) with or without NEt_3 (7.98 mmol)

Table 5. Crystallographic data for **1a**, **4a**, **5a**, and **7a**

	1a	**4a**	**5a**	**7a**
Emprical formula	$C_{28}H_{30}Cl_2CuN_6O_{11}$	$C_{32}H_{29}Cl_2CuN_7O_9$	$C_{34}H_{34}Cl_2CuN_6O_9$	$C_{22}H_{20}Cl_2CuN_4O_9$
Molecular mass	761.02	790.06	805.11	618.87
Crystal system	monoclinic	triclinic	triclinic	triclinic
Space group	$P2_1/c$	$P\bar{1}$	$P\bar{1}$	$P\bar{1}$
a (Å)	15.5495(7)	10.1156(5)	10.2008(14)	8.8186(1)
b (Å)	10.1854(4)	11.6347(6)	11.7156(15)	10.6142(2)
c (Å)	20.5931(9)	16.9338(9)	16.628(2)	15.0084(4)
α [°]	90	78.495(1)	72.383(2)	88.644(1)
β [°]	101.532(1)	76.100(1)	77.804(2)	75.102(1)
γ [°]	90	64.906(1)	70.921(2)	67.897(2)
V (Å^3)	3195.7(2)	1741.19(16)	1776.0(4)	1243.63(4)
Z	4	2	2	2
F(000)	1564	810	830	630
$D_{calcd.}$ [Mg·m^{-1}]	1.582	1.507	1.506	1.640
μ(Mo-K_α) [mm^{-1}]	0.920	0.844	0.829	1.14
Crystal size [mm]	0.10 × 0.08 × 0.05	0.40 × 0.25 × 0.20	0.25 × 0.18 × 0.10	0.40 × 0.35 × 0.15
Diffractometer	Siemens SMART CCD	Siemens SMART CCD	Siemens SMART CCD	Bruker Kappa CCD
θ range [°]	1.34−28.32	1.94−28.29	1.90−28.29	27.52
T_{max}, T_{min}	0.98078, 0.83846	0.95739, 0.80920	0.96645, 0.85317	0.746, 0.682
hkl range	$-20 \le h \le 20$, $-13 \le k \le 13$, $-27 \le l \le 23$	$-13 \le h \le 13$, $-15 \le k \le 15$, $-22 \le l \le 22$	$-13 \le h \le 13$, $-15 \le k \le 15$, $-21 \le l \le 22$	$-10 \le h \le 11$, $-13 \le k \le 13$, $-19 \le l \le 19$
No. of reflns. measd.	20477	18424	18936	12335
No. of unique reflns.	7763	8233	8415	5915
No. of reflns. obsd.	3514($I > 2\sigma$)	5172($I > 2\sigma$)	3868($I > 2\sigma$)	4564($I > 3\sigma$)
R_{int}	0.0658	0.0411	0.0623	0.036
No. of param./restraints	427/0	460/0	469/0	344/0
R, R_w	0.0649, 0.1765	0.0743, 0.1919	0.0754, 0.1764	0.047, 0.090
Max./min. Δρ [e·Å^{-3}]	1.281/-0.830	0.914/-0.488	1.108/-0.337	0.48/-0.54
Goodness-of-fit	0.928	1.023	0.930	1.155

was added to a mixture of $[Cu(CH_3CN)_4](ClO_4)$ (26.1 mg, 0.0798 mmol) and tridentate ligand (0.0798 mmol) in CH_2Cl_2/CH_3CN (8:2, 10 mL) under N_2. The reaction solution was stirred under an O_2 atmosphere at room temperature and was monitored by checking the UV/Vis absorption in the region of 300 nm to 800 nm. After the absorption peaks stopped growing, the reaction mixture was worked up as described above, yielding 3,3′,5,5′-tetra-*tert*-butyl-2,2′-biphenol, and/or 3,5-di-*tert*-butyl-*o*-quinone.

X-ray Crystallographic Study: Details of crystal data and intensity collection are summarized in Table 5, using Siemens Smart-CCD or Bruker−Kappa CCD diffractometers. Intensity data [θ/2θ scan] were collected at ca. 298 K and corrected for Lorentz and polarization effects and absorption. The structures were solved by direct methods using the SIR92 for (**7a**) and SHELXS-97 for the rest. The hydrogen atoms included in the refinement were located in succeeding difference Fourier syntheses or with ideal positions after the non-hydrogen atoms were refined anisotropically. CCDC-217573 to -217576 contains the supplementary crystallographic data for this paper. These data can be obtained free of charge at www.ccdc.cam.ac.uk/conts/retrieving.html [or from the Cambridge Crystallographic Data Centre, 12 Union Road, Cambridge CB2 1EZ, UK; Fax: (internat.) + 44-1223-336-033; E-mail: deposit@ccdc.cam.ac.uk].

Acknowledgments

Financial support form the National Science Council of the Republic of China (NSC89-2113-M-003-018) is gratefully acknowledged. Our gratitude also goes to the Academic Paper Editing Clinic, NTNU.

[1] K. A. Magnus, H. Ton-That, J. E. Carpenter, in: *Bioinorganic Chemistry of Copper* (Ed.: K. D. Karlin, Z. Tyeklar), Chapman & Hall, New York, **1993**, 143−150.
[2] K. A. Magnus, H. Ton-That, J. E. Carpenter, *Chem. Rev.* **1994**, *94*, 727−735.
[3] E. I. Solomon, M. J. Baldwin, M. D. Lowery, *Chem. Rev.* **1992**, *92*, 521−542.
[4] E. I. Solomon, U. M. Sundaram, T. E. Machonkin, *Chem. Rev.* **1996**, *96*, 2563−2605.
[5] N. Kitajima, K. Fujisawa, C. Fujimoto, Y. Moro-Oka, S. Hashimoto, T. Kitagawa, K. Toriumi, K. Tatsumi, A. Nakamura, *J. Am. Chem. Soc.* **1992**, *114*, 1277−1291.
[6] E. Pidcock, S. DeBeer, H. V. Obias, B. Hedman, K. O. Hodgson, K. D. Karlin, E. I. Solomon, *J. Am. Chem. Soc.* **1999**, *121*, 1870−1878.
[7] M. Kodera, K. Katayama, Y. Tachi, K. Kano, S. Hirota, S. Fujinami, M. Suzuki, *J. Am. Chem. Soc.* **1999**, *121*, 11006−11007.
[8] Z. Hu, G. N. George, S. M. Gorun, *Inorg. Chem.* **2001**, *40*, 4812−4813.
[9] S. Mahapatra, J. A. Halfen, E. C. Wilkinson, G. Pan, X. Wang, V. G. Young, Jr., C. J. Cramer, L. Que, Jr., W. B. Tolman, *J. Am. Chem. Soc.* **1996**, *118*, 11555−11574.
[10] J. A. Halfen, S. Mahapatra, E. C. Wilkinsin, S. Kaderli, V. G. Young, Jr., L. Que, Jr., A. D. Zuberbuhler, W. B. Tolman, *Science* **1996**, *271*, 1397−1400.
[11] S. Mahapatra, V. G. Young, Jr., S. Kaderli, A. D. Zuberbuhler,

W. B. Tolman, *Angew. Chem.* **1997**, *109*, 125−127; *Angew. Chem. Int. Ed. Engl.* **1997**, *36*, 130−133.
[12] N. W. Aboelella, E. A. Lewis, A. M. Reynolds, W. W. Brennessel, C. J. Cramer, W. B. Tolman, *J. Am. Chem. Soc.* **2002**, *124*, 10660−10661.
[13] D. J. E. Spencer, A. M. Reynolds, P. L. Holland, B. A. Jazdzewski, C. Duboc-Toia, L. Le Pape, S. Yokota, Y. Tachi, S. Itoh, W. B. Tolman, *Inorg. Chem.* **2002**, *41*, 6307−6321.
[14] V. Mahadevan, Z. Hou, A. P. Cole, D. E. Root, T. K. Lal, E. I. Solomon, T. D. P. Stack, *J. Am. Chem. Soc.* **1997**, *119*, 11996−11997.
[15] P. P. Paul, Z. Tyeklar, R. R. Jacobson, K. D. Karlin, *J. Am. Chem. Soc.* **1991**, *113*, 5322−5332.
[16] M. S. Nasir, B. I. Cohen, K. D. Karlin, *J. Am. Chem. Soc.* **1992**, *114*, 2482−2494.
[17] K. D. Karlin, M. S. Nasir, B. I. Cohen, R. W. Cruse, S. Kaderli, A. D. Zuberbuhler, *J. Am. Chem. Soc.* **1994**, *116*, 1324−1336.
[18] E. Pidcock, H. V. Obias, C. X. Zhang, K. D. Karlin, E. I. Solomon, *J. Am. Chem. Soc.* **1998**, *120*, 7841−7847.
[19] W. B. Tolman, *Acc. Chem. Res.* **1997**, *30*, 227−237.
[20] J. Cahoy, P. L. Holland, W. B. Tolman, *Inorg. Chem.* **1999**, *38*, 2161−2168.
[21] L. Que, Jr., W. B. Tolman, *Angew. Chem.* **2002**, *114*, 1160−1185; *Angew. Chem. Int. Ed.* **2002**, *41*, 1114−1137.
[22] H.-C. Liang, C. X. Zhang, M. J. Henson, R. D. Sommer, K. R. Hatwell, S. Kaderli, A. D. Zuberbuehler, A. L. Rheingold, E. I. Solomon, K. D. Karlin, *J. Am. Chem. Soc.* **2002**, *124*, 4170−4171.
[23] V. Mahadevan, M. J. Henson, E. I. Solomon, T. D. P. Stack, *J. Am. Chem. Soc.* **2000**, *122*, 10249−10250.
[24] M. J. Henson, P. Mukherjee, D. E. Root, T. D. P. Stack, E. I. Solomon, *J. Am. Chem. Soc.* **1999**, *121*, 10332−10345.
[25] L. M. Mirica, M. Vance, D. J. Rudd, B. Hedman, K. O. Hodgson, E. I. Solomon, T. D. P. Stack, *J. Am. Chem. Soc.* **2002**, *124*, 9332−9333.
[26] V. Mahadevan, J. L. DuBois, B. Hedman, K. O. Hodgson, T. D. P. Stack, *J. Am. Chem. Soc.* **1999**, *121*, 5583−5584.
[27] M. Palaniandavar, T. Pandiyan, M. Lakshminarayanan, H. Manohar, *J. Chem. Soc., Dalton Trans.* **1995**, 455−461.
[28] L. Casella, O. Carugo, M. Gullotti, S. Doldi, M. Frassoni, *Inorg. Chem.* **1996**, *35*, 1101−1113.
[29] Y. Nishida, K. Takashi, *J. Chem. Soc., Dalton Trans.* **1988**, 691−699.
[30] B. J. Hathaway, in: *Comprehensive Coordination Chemistry* (Ed.: G. Wilkinson, R. D. Gillard, J. A. McCleverty), vol. 5, Pergamon Press, Oxford, **1987**, pp. 594−774.
[31] B. J. Hathaway, A. A. G. Tomlison, *Coord. Chem. Rev.* **1970**, *5*, 1−142.
[32] U. Sakaguchi, A. W. Addison, *J. Chem. Soc., Dalton Trans.* **1979**, 600−608.
[33] N. Kitajima, T. Koda, Y. Iwata, Y. Moro-oka, *J. Am. Chem. Soc.* **1990**, *112*, 8833−8839.
[34] H. V. Obias, Y. Lin, N. N. Murthy, E. Pidcock, E. I. Solomon, M. Ralle, N. J. Blackburn, Y.-M. Neuhold, A. D. Zuberbuhler, K. D. Karlin, *J. Am. Chem. Soc.* **1998**, *120*, 12960−12961.
[35] J. A. Halfen, V. G. Young, Jr., W. B. Tolman, *Inorg. Chem.* **1998**, *37*, 2102−2103.
[36] L. Casella, M. Gullotti, R. Radaelli, P. Di Gennaro, *J. Chem. Soc., Chem. Commun.* **1991**, 1611−1612.
[37] L. Casella, E. Monzani, M. Gullotti, D. Cavagnino, G. Cerina, L. Santagostini, R. Ugo, *Inorg. Chem.* **1996**, *35*, 7516−7525.
[38] E. Monzani, L. Quinti, A. Perotti, L. Casella, M. Gullotti, L. Randaccio, S. Geremia, G. Nardin, P. Faleschini, G. Tabbi, *Inorg. Chem.* **1998**, *37*, 553−562.
[39] L. Santagostini, M. Gullotti, E. Monzani, L. Casella, R. Dillinger, F. Tuczek, *Chem. Eur. J.* **2000**, *6*, 519−522.
[40] S. Itoh, H. Kumei, M. Taki, S. Nagatomo, T. Kitagawa, S. Fukuzumi, *J. Am. Chem. Soc.* **2001**, *123*, 6708−6709.
[41] H. P. Berends, D. W. Stephan, *Inorg. Chim. Acta* **1984**, *93*, 173−178.
[42] G. Batra, P. Mathur, *Inorg. Chem.* **1992**, *31*, 1575−1580.
[43] Y. Kikugawa, *Synthesis* **1981**, 124−125.
[44] D. Nanty, M. Laurent, M. A. Khan, M. T. Ashby, *Acta Crystallogr., Sect. C* **2000**, *56*, 35−36.

Received September 9, 2003
Early View Article
Published Online April 1, 2004

